OL Organic Letters

pubs.acs.org/OrgLett Letter

Strategic Construction of Ethene-Bridged BODIPY Arrays with Absorption Bands Reaching the Near-Infrared II Region

Qinghua Wu, Zhengxin Kang, Qingbao Gong, Xing Guo, Hua Wang, Dandan Wang, Lijuan Jiao,* and Erhong Hao*

Cite This: https://dx.doi.org/10.1021/acs.orglett.0c02704 Read Online

ACCESS | Metrics & More | Article Recommendations | Supporting Information

ABSTRACT: An efficient strategy for the controllable synthesis of BODIPY arrays based on the Stille cross-coupling reaction has been developed, from which a family of well-defined ethene-bridged BODIPY arrays from dimer to hexamer was synthesized. These arrays showed strong absorptions reaching the near-infrared II (NIR II, 1000−1700 nm) region with maxima tunable from 702 nm (dimer) to 1114 nm (hexamer) and possessed efficient light-harvesting capabilities, excellent photostability, and good photothermal conversion abilities under NIR light irradiation.

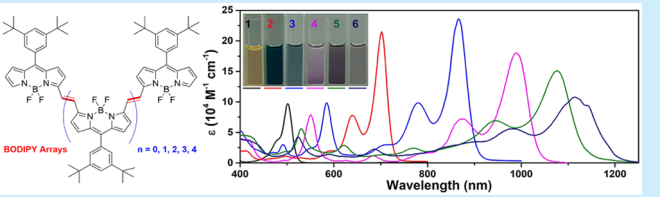

Highly stable, small organic molecules with strong absorption beyond 800 nm have recently received much attention because of their practical applications as optoelectronic materials,[1] in bioimaging,[2] and as theranostics reagents.[3] A conventional approach to obtain such low-band-gap dyes is the introduction of a push−pull motif along the molecular long axis (for example, **ICG** and **NIRb**, shown in Figure 1a).[4] Another straightforward strategy is the extension of π-conjugation. To maximize π-overlap, it is necessary to hold the π-systems coplanar within a rigid tapelike framework by fusing the units edge-to-edge (Figure 1b).[5−7] For example, the [*n*]acene series,[5] fused isoindigo ribbons,[6] and fully conjugated porphyrin tapes (**PTs**) and expanded porphyrinoids[7] are noticeable polycyclic aromatics with low, tunable band gaps. However, these approaches typically encounter serious problems, such as a challenging synthesis, chemical instability, and poor solubility caused by the resulting planar structures.

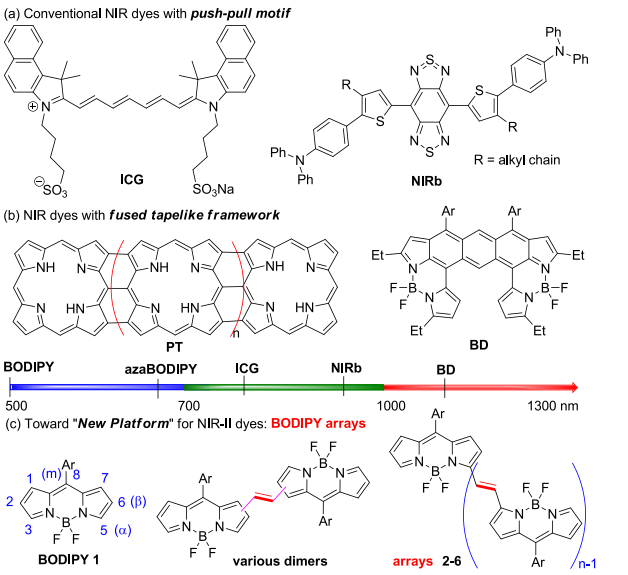

Figure 1. Schematic of the design strategies for NIR dyes based on (a) the push−pull motifs and (b) the π-extended fused tapelike framework. (c) Structure and numbering of BODIPY **1**, possible ethene-linked BODIPY dimers, and arrays **2**−**6** in this work.

Boron dipyrromethenes (BODIPYs), as a class of emerging small-molecule fluorophores, are intriguing building units for NIR dyes because of their excellent stability arising from the strongly electron-withdrawing BF_2 group and their intense absorption.[8] Many BODIPY-based NIR dyes,[9−12] including several well-designed fused BODIPY dimers[10] and linear BODIPY oligomers,[12] have been synthesized; however, their main absorption bands mostly fall in the range of <800 nm. A sole example of fused BODIPY dimers, **BD** (Figure 1b) with diradical character, was reported by Wu and coworkers[10i] and showed strong absorption bands beyond 1100 nm. Nevertheless, the synthesis of fused dimers is difficult, and extension to the higher fused BODIPY homologues is extremely challenging to achieve due to the synthetic inaccessibility. Recently, versatile and rapid access to various chain lengths of nonconjugated, ethylene-bridged BODIPY motifs (up to

Received: August 13, 2020

https://dx.doi.org/10.1021/acs.orglett.0c02704
Org. Lett. XXXX, XXX, XXX−XXX

octamer) was discovered by Werz and coworkers.[12e] These nonconjugated oligo-BODIPYs showed interesting *J*-type excitonic coupling, outstandingly high attenuation coefficients, and intense fluorescence.

Inspired by these results, we wondered whether a simple ethene-bridged BODIPY dimer without steric hindrance may also exhibit effective π-conjugation by mainly adopting a coplanar conformation. Extension to the higher ethene-bridged BODIPY arrays may provide a simple way to build dyes with intense and tunable NIR absorption. In addition, the flexible linkage permits the free rotation of each BODIPY unit in the excited state, deactivating excited states through the nonradiative channel[13] and possibly converting absorbed photons into heat.[9e] It should be noted that ethene-bridged BODIPY dimers and trimers with steric encumbrance have been reported for promising theranostics reagents.[12a,d]

Herein we report an efficient cross-coupling strategy of α-chlorinated BODIPYs to give a series of ethene-bridged BODIPY arrays, including the first structurally characterized dimer to hexamer. These arrays showed absorption maxima tunable from 702 (dimer) to 1114 nm (hexamer) and possessed efficient light-harvesting capabilities and excellent photostability. This research is of fundamental interest for studying the structure−property relationships of ultraphotostable NIR photosensitizers as photothermal reagents, which are highly desirable for biomedical applications.

Initially, theoretical calculations were conducted on the six possible ethene-linked BODIPY dimers (Scheme S1 in the Supporting Information (SI)) to examine their geometric and electronic properties (Figures S1 and S2 and Table S1). Among them, $\alpha-\alpha$, $\alpha-\beta$, and $\beta-\beta$ ethene-linked BODIPY dimers showed coplanar conformations, and the dihedral angles between adjacent dipyrrin planes were 4.3, 2.9, and 4.5°, respectively. In contrast, $\alpha-m$, $\beta-m$, and $m-m$ ethene-linked BODIPY dimers have relatively large dihedral angles of 15.2, 39.0, and 73.1°, respectively (Figure S1). Moreover, a significant difference is shown in the energy levels between these ethene-linked BODIPY dimers, in which the $\alpha-\alpha$-linked dimer has the lowest band gap of 2.09 eV. Importantly, $\alpha-\alpha$ and $\alpha-\beta$ dimers gave the most red-shifted absorption, with maxima at 621 nm by TDDFT calculations (Figure S2 and Table S2), whereas only the HOMOs and LUMOs of $\alpha-\alpha$ and $\beta-\beta$ dimers are delocalized across the entire molecules.

In conjunction with the previously described results in the favor of $\alpha-\alpha$-linked dimer, we then carried out calculations on the $\alpha-\alpha$-linked higher arrays **3**−**6**, which all showed small dihedral angles (1.17−5.15°) between adjacent dipyrrin planes (Table S1). The calculated energy levels of arrays at the B3LYP/6-31G(d) level are effective at decreasing their LUMO levels (−3.24, −3.42, −3.50, −3.56, and −3.59 eV from dimer **2** to hexamer **6**, respectively) and increasing their HOMO levels (−5.39, −5.10, −4.98, −4.91, and −4.87 eV from dimer **2** to hexamer **6**, respectively). The HOMOs and LUMOs are delocalized across the entire molecules for monomer **1** to pentamer **5** (Figure S3), whereas those of hexamer **6** are mainly delocalized in the central four BODIPY units. Arrays **2**−**6** showed calculated absorption maxima of 621, 809, 938, 1077, and 1169 nm, respectively, where the corresponding monomer **1** absorbs only ~406 nm (Table S3). The S_1 states of these arrays are mainly assigned to the electronic transitions of HOMO → LUMO. Furthermore, the oscillator strength enhancement of the corresponding transitions with the increase in the BODIPY units, which induces the increase in molar absorption coefficients, was observed, suggesting the strong light-harvesting ability of these BODIPY arrays.

Next, on the basis of our recently reported α-chlorination of BODIPY,[14] we developed an efficient method for the synthesis of BODIPY arrays **2**−**6**, as depicted in Schemes 1 and 2. The

Scheme 1. Synthesis of 2, 3, and Chlorinated Derivatives[a]

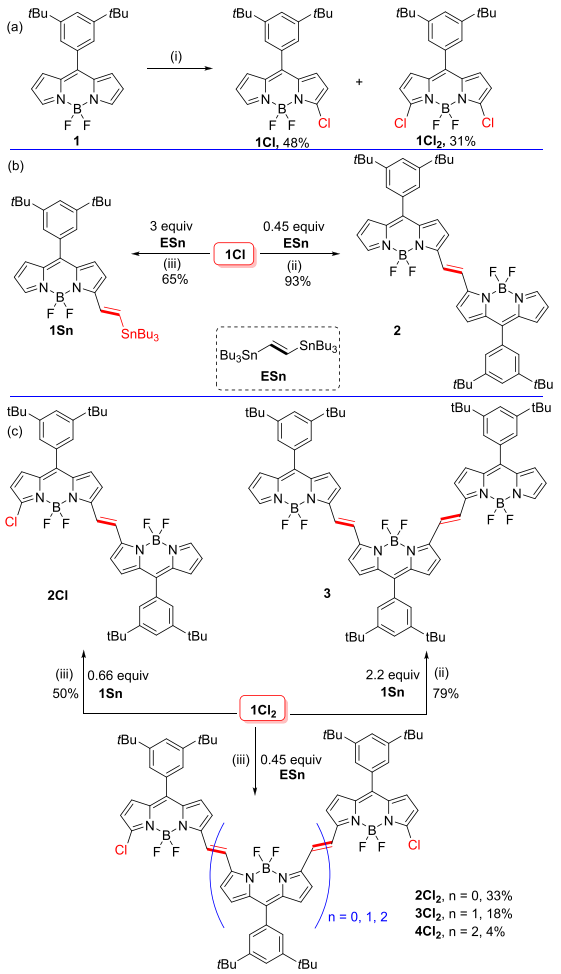

[a]Reaction conditions: (i) $CuCl_2 \cdot 2H_2O$, acetonitrile, 80 °C. (ii) Pd_2dba_3, P(*o*-tol)$_3$, toluene, 110 °C. (iii) Pd_2dba_3, P(*o*-tol)$_3$, toluene, rt.

key intermediates **1Cl** and **1Cl$_2$** were first synthesized and were used to build ethene-bridged arrays through the Stille coupling reaction (Scheme 1a). The palladium-catalyzed Stille coupling reaction was selected because it has several advantages, such as mild reaction conditions and high yields of target products.[15] We first screened several different conditions for the Stille coupling between **1Cl** and *trans*-1,2-bis(tributylstannyl)ethene (**ESn**). Pd_2dba_3 and the ligand P(*o*-tol)$_3$ were found to be an efficient catalyst system for this reaction. Using this optimized condition, the Stille coupling of **1Cl** with 0.45 equiv of **ESn** gave the symmetrical dimer **2** in 93% yield (Scheme 1b) in refluxing toluene. Both the reaction temperature and the amount of substrates were used to control the selectivity of the Stille reaction. At room temperature, this coupling between **1Cl** and 3 equiv of **ESn** produced **1Sn** in 65% yield (Scheme 1b).

Trimer **3** was then obtained in 79% yield from the cross-coupling reaction between **1Cl$_2$** and 2.2 equiv of **1Sn** (Scheme 1c) using the above Stille coupling condition in refluxing

https://dx.doi.org/10.1021/acs.orglett.0c02704
Org. Lett. XXXX, XXX, XXX−XXX

Scheme 2. Synthesis of 4−6[a]

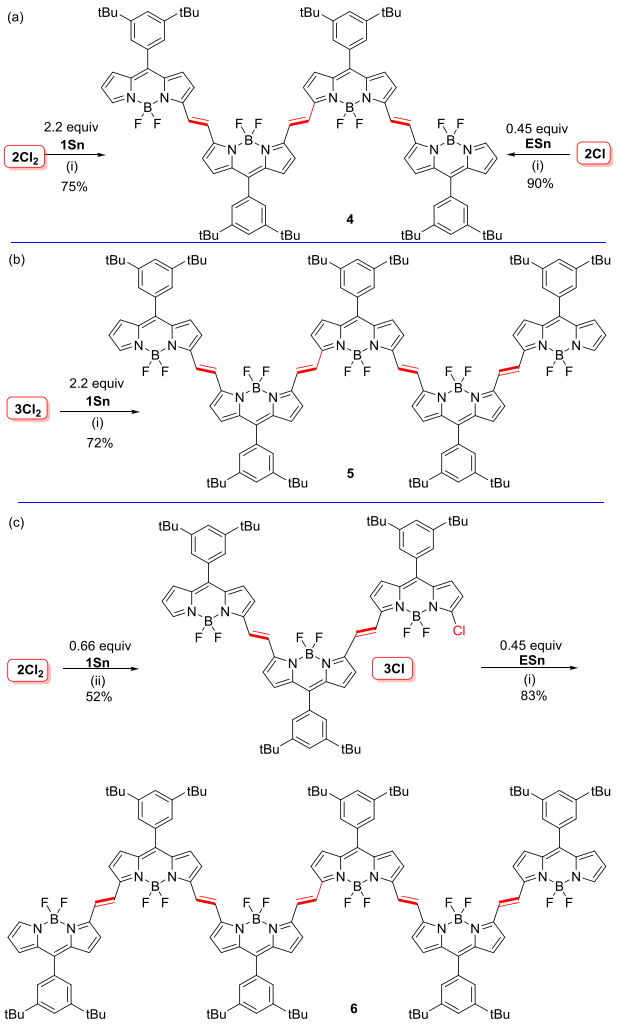

[a]Reaction conditions: (i) Pd_2 dba_3, P(*o*-tol)$_3$, toluene, 110 °C. (ii) Pd_2 dba_3, P(*o*-tol)$_3$, toluene, rt.

toluene. Similarly, when only 0.66 equiv of **1Sn** was used to react with **1Cl$_2$** at room temperature in toluene, dimer **2Cl** was isolated in 50% yield as the main product (Scheme 1c). Interestingly, when **1Cl$_2$** was reacted with 0.45 equiv of **ESn** in toluene at room temperature for 24 h (Scheme 1c), a mixture of chlorinated oligomers **2Cl$_2$**, **3Cl$_2$**, and **4Cl$_2$** was isolated in one pot in 33, 18, and 4% yield, respectively.

Tetramer **4** was synthesized by two different methods from dimers **2Cl** and **2Cl$_2$** (Scheme 2a), respectively. By adopting the same strategy as that for dimer **2**, **4** was obtained in 90% yield from the Stille coupling of **2Cl** and 0.45 equiv of **ESn** in refluxing toluene. Moreover, tetramer **4** was also constructed in 75% yield from dichloroBODIPY dimer **2Cl$_2$** and 2.2 equiv of **1Sn**, similar to the synthesis of trimer **3**. Using this strategy, pentamer **5** was synthesized in 72% yield in the Stille coupling reaction between dichloroBODIPY trimer **3Cl$_2$** and 2.2 equiv of **1Sn** (Scheme 2b). Finally, hexamer **6** was synthesized in 83% yield from the Stille coupling of trimer **3Cl** and 0.45 equiv of **ESn** (Scheme 2c). The key intermediate trimer **3Cl** was obtained as the major product in 52% yield from the one-fold Stille coupling of **1Sn** and an excess amount of dichloroBODIPY **2Cl$_2$** at room temperature.

The high-resolution MALDI-TOF mass spectra of **2−6** reveal a single species with precise isotopic distribution patterns that are in good agreement with the calculations (SI). The chemical structures and the purity of arrays **2−6** were also confirmed by NMR spectroscopy. The structure of **2Cl$_2$** was unambiguously elucidated by single-crystal X-ray diffraction (Figure S5 and Table S4), revealing its highly planar structure, including the ethene linkage. The deviation from the mean plane, which consisted of the two BODIPY units and the ethene moiety, was only 0.087 Å. The length of the bond (d_1) between the BODIPY unit and the ethene linkage was 1.43 Å, which is shorter than the standard C_{sp^2}−C_{sp^2} single-bond length. The ethene C=C bond (d_2) length was 1.34 Å. These data indicate the well-extended conjugation between the BODIPY unit and the ethene linkage in this dimer.

Figure 2a shows the absorption spectra of dyes **1−6** in toluene, which have absorption maxima of 500, 702, 866, 990,

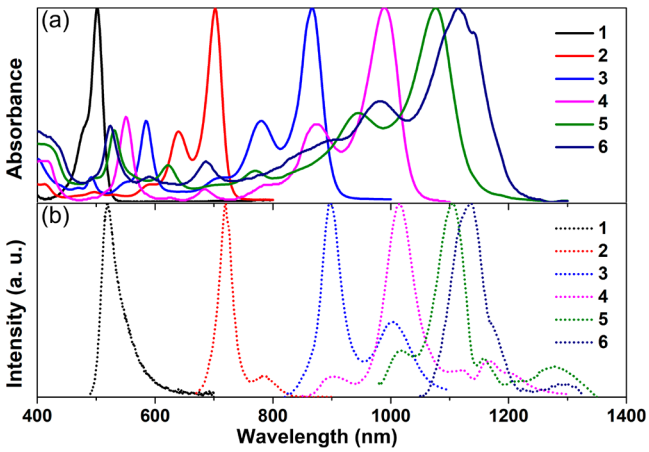

Figure 2. (a) Normalized absorption and (b) emission profile of **1−6** in toluene.

1076, and 1114 nm, respectively. The lowest energy bands were substantially shifted to the low-energy region with the increase in BODIPY units, indicating the effective expansion of π-conjugation upon oligomerization. With the increase in the conjugation chain, the fwhm (full width at half-maximum) values were significantly increased (from 30 nm for dimer **2** to 111 nm for hexamer **6**) in toluene. Importantly, the molar absorption coefficients of arrays **2−6** also have significant enhancement (Table 1) in comparison with that of **1**. Among them, trimer **3** gives the highest molar absorption coefficient of 248 000 M^{-1} cm^{-1} at 856 nm, indicating the strong light-harvesting ability of these BODIPY arrays. The λ_{abs}(max) and

Table 1. Photophysical Properties of 1−6 in Toluene at Room Temperature

arrays	λ_{max} (nm)	ε (M^{-1} cm^{-1})	λ_{em} (nm)	ϕ (%)[a]	ss (cm^{-1})[b]
1	501	97000	520	38	729
2	702, 639 (sh)[c]	215000	720	24	356
3	866, 781 (sh)	236000	895	1.5	374
4	990, 873 (sh)	180000	1015	0.7	249
5	1076, 948 (sh)	151000	1106	0.3	252
6	1114, 983 (sh)	108000	1136	0.2	174

[a]Relative fluorescence quantum yields. [b]Stokes shifts. [c]sh means the shoulder peak.

https://dx.doi.org/10.1021/acs.orglett.0c02704
Org. Lett. XXXX, XXX, XXX−XXX

λ_{em}(max) values for arrays **2**−**4** (Figures S6−S8) are hypsochromically shifted with increasing solvent polarity and decreasing polarizability, similar to those of typical BODIPYs.[8e] Arrays **2**−**6** also show deep NIR and NIR-II emission, with the maximal peaks at 720, 895, 1015, 1106, and 1136 nm in toluene (Figure 2b), respectively. The Stokes shift tends to be smaller with the increase in the conjugation chain (Table 1), indicating smaller geometric rearrangements upon excitation in higher oligomers.[12a] The fluorescence quantum yields gradually decrease with the increase in BODIPY units. Dimer **2** shows a decent fluorescence quantum yield of 24%, and trimer **3** exhibits weak emission with a fluorescence quantum yield of 1.5%. Arrays **4**−**6** all give interesting NIR-II emission in the range of 1000−1300 nm; however, their fluorescence quantum yields were <1% in toluene. The quenching of fluorescence might be due to the rotation of BODIPY units around ethene linkages in the excited state.

Arrays **3**−**6** exhibit weak emission and have strong absorption above 800 nm, which falls within the wavelength range of the commercial NIR laser source. Therefore, the photothermal conversion properties of **3**−**6** were investigated in toluene (50 μg/mL) under 808 or 980 nm laser irradiation with clinically approved indocyanine green (**ICG**) as a reference. As shown in Figures S10−S14, the solution temperatures showed rapid increases under continuous laser irradiation and then gradually decreased to room temperature after the laser irradiation was stopped. All dyes showed no degradation after five cycles of heating and cooling under continuous laser irradiation. The photothermal conversion efficiencies were in the range of 30.4−34.8% for arrays **3**−**5**, whereas hexamer **6** showed a photothermal conversion efficiency of 18.2% under 980 nm laser irradiation.[16]

Encouraged by these promising photothermal properties, trimer **3** was selected to prepare water-soluble nanoparticles by encapsulating in well-known Pluronic F127 block copolymers.[17] The formation of micelles was confirmed by dynamic light scattering, of which the hydrodynamic sizes were ∼160 nm (Figure S15). The resultant **3NPs** exhibited excellent water solubility and slightly red-shifted absorption when compared with that of trimer **3** dissolved in DMF (Figure S16a). When exposed to laser irradiation (808 nm, 1.0 W/cm^2), the **3NPs** solution in PBS showed obvious concentration-dependent photothermal conversions (Figure S16b). A net temperature increment of ∼55 °C at a concentration of 40 μg/mL after 300 s of laser exposure was obtained. Furthermore, an obvious laser intensity-dependent temperature enhancement of **3NPs** was observed (Figure S16c). The calculated photothermal conversion efficiency of **3NPs** in PBS solution was 56.8% (Figure S16d,e). While under the same conditions, **ICG** gave a photothermal conversion efficiency of only 23% (Figure S17). Moreover, the photothermal performance of **3NPs** did not change from five repeated heating/cooling cycles (with 5 min of laser exposure each cycle), which was attributed to the great photothermal stability of trimer **3** (Figure S16f). The much higher stability of **3NPs** under irradiation compared with that of **ICG**, together with their high photothermal conversion efficiency and large molar absorption coefficient, enable them to be attractive candidates as NIR dyes for biorelated applications.

In summary, we have presented a novel, facile cross-coupling strategy for the controllable synthesis of well-conjugated BODIPY arrays, in which an almost coplanar structure of the BODIPY units and the ethene linkage were obtained. Intense NIR-I and II absorption as well as emission, extraordinary photostability, and high photothermal conversion efficiencies enable these BODIPY arrays to be new NIR materials for potential biorelated applications. This finding indicated how conjugated BODIPY arrays could be a simple yet efficient method to access dyes with tunable absorption bands reaching the NIR II region.

■ ASSOCIATED CONTENT

Supporting Information

The Supporting Information is available free of charge at https://pubs.acs.org/doi/10.1021/acs.orglett.0c02704.

Experimental details, additional photophysical data, DFT calculations, characterization and properties of nanoparticles, and NMR and HRMS spectra (PDF)

Accession Codes

CCDC 1991866 contains the supplementary crystallographic data for this paper. These data can be obtained free of charge via www.ccdc.cam.ac.uk/data_request/cif, or by emailing data_request@ccdc.cam.ac.uk, or by contacting The Cambridge Crystallographic Data Centre, 12 Union Road, Cambridge CB2 1EZ, UK; fax: +44 1223 336033.

■ AUTHOR INFORMATION

Corresponding Authors

Lijuan Jiao − *The Key Laboratory of Functional Molecular Solids, Ministry of Education, School of Chemistry and Materials Science, Anhui Normal University, Wuhu 241002, China;* orcid.org/0000-0002-3895-9642; Email: jiao421@ahnu.edu.cn

Erhong Hao − *The Key Laboratory of Functional Molecular Solids, Ministry of Education, School of Chemistry and Materials Science, Anhui Normal University, Wuhu 241002, China;* orcid.org/0000-0001-7234-4994; Email: haoehong@ahnu.edu.cn

Authors

Qinghua Wu − *The Key Laboratory of Functional Molecular Solids, Ministry of Education, School of Chemistry and Materials Science, Anhui Normal University, Wuhu 241002, China;* orcid.org/0000-0002-7252-7990

Zhengxin Kang − *The Key Laboratory of Functional Molecular Solids, Ministry of Education, School of Chemistry and Materials Science, Anhui Normal University, Wuhu 241002, China*

Qingbao Gong − *The Key Laboratory of Functional Molecular Solids, Ministry of Education, School of Chemistry and Materials Science, Anhui Normal University, Wuhu 241002, China*

Xing Guo − *The Key Laboratory of Functional Molecular Solids, Ministry of Education, School of Chemistry and Materials Science, Anhui Normal University, Wuhu 241002, China*

Hua Wang − *The Key Laboratory of Functional Molecular Solids, Ministry of Education, School of Chemistry and Materials Science, Anhui Normal University, Wuhu 241002, China*

Dandan Wang − *The Key Laboratory of Functional Molecular Solids, Ministry of Education, School of Chemistry and Materials Science, Anhui Normal University, Wuhu 241002, China*

Complete contact information is available at:

https://dx.doi.org/10.1021/acs.orglett.0c02704
Org. Lett. XXXX, XXX, XXX−XXX

https://pubs.acs.org/10.1021/acs.orglett.0c02704

Notes

The authors declare no competing financial interest.

■ ACKNOWLEDGMENTS

This work is supported by the National Nature Science Foundation of China (grants 21672007, 21672006, 21871006, and 21971004). The numerical calculations in this paper have been done on the supercomputing system in the Supercomputing Center of The University of Science and Technology of China.

■ REFERENCES

(1) (a) Cao, Y.; Dou, J.; Zhao, N.; Zhang, S.; Zheng, Y.; Zhang, J.; Wang, J.; Pei, J.; Wang, Y. *Chem. Mater.* **2017**, *29*, 718−725. (b) Liu, C.; Wang, K.; Gong, X.; Heeger, A. *Chem. Soc. Rev.* **2016**, *45*, 4825−4846.

(2) (a) Wu, D.; Sedgwick, A.; Gunnlaugsson, T.; Akkaya, E.; Yoon, J.; James, T. *Chem. Soc. Rev.* **2017**, *46*, 7105−7123. (b) Yang, Z.; Sharma, A.; Qi, J.; Peng, X.; Lee, D.; Hu, R.; Lin, D.; Qu, J.; Kim, J. *Chem. Soc. Rev.* **2016**, *45*, 4651−4667. (c) Lei, Z.; Li, X.; Luo, X.; He, H.; Zheng, J.; Qian, X.; Yang, Y. *Angew. Chem., Int. Ed.* **2017**, *56*, 2979−2983. (d) Zhao, W.; Carreira, E. M. *Angew. Chem., Int. Ed.* **2005**, *44*, 1677−1679.

(3) (a) Zhao, L.; Liu, Y.; Xing, R.; Yan, X. *Angew. Chem., Int. Ed.* **2020**, *59*, 3793−3801. (b) Nie, L.; Chen, X. *Chem. Soc. Rev.* **2014**, *43*, 7132−7170.

(4) (a) Antaris, A. L.; Chen, H.; Cheng, K.; Sun, Y.; Hong, G.; Qu, C.; Diao, S.; Deng, Z.; Hu, X.; Zhang, B.; Zhang, X.; Yaghi, O. K.; Alamparambil, Z. R.; Hong, X.; Cheng, Z.; Dai, H. *Nat. Mater.* **2016**, *15*, 235−242. (b) Lei, Z.; Sun, C.; Pei, P.; Wang, S.; Li, D.; Zhang, X.; Zhang, F. *Angew. Chem., Int. Ed.* **2019**, *58*, 8166−8171. (c) Yang, Q.; Hu, Z.; Zhu, S.; Ma, R.; Ma, H.; Ma, Z.; Wan, H.; Zhu, T.; Jiang, Z.; Liu, W.; Jiao, L.; Sun, H.; Liang, Y.; Dai, H. *J. Am. Chem. Soc.* **2018**, *140*, 1715−1724. (d) Liu, S.; Zhou, X.; Zhang, H.; Ou, H.; Lam, J.; Liu, Y.; Shi, L.; Ding, D.; Tang, B. *J. Am. Chem. Soc.* **2019**, *141*, 5359−5368.

(5) Shen, S.; Tatchen, J.; Sanchez-Garcia, E.; Bettinger, H. *Angew. Chem., Int. Ed.* **2018**, *57*, 10506−10509.

(6) Jiang, Y.; Zheng, X.; Deng, Y.; Tian, H.; Ding, J.; Xie, Z.; Geng, Y.; Wang, F. *Angew. Chem., Int. Ed.* **2018**, *57*, 10283−10287.

(7) (a) Tsuda, A.; Osuka, A. *Science* **2001**, *293*, 79−82. (b) Diev, V.; Hanson, K.; Zimmerman, J.; Forrest, S.; Thompson, M. *Angew. Chem., Int. Ed.* **2010**, *49*, 5523−5526. (c) Wang, Y.; Kai, H.; Ishida, M.; Gokulnath, S.; Mori, S.; Murayama, T.; Muranaka, A.; Uchiyama, M.; Yasutake, Y.; Fukatsu, S.; Notsuka, Y.; Yamaoka, Y.; Hanafusa, M.; Yoshizawa, M.; Kim, G.; Kim, D.; Furuta, H. *J. Am. Chem. Soc.* **2020**, *142*, 6807−6813. (d) Shimomura, K.; Kai, H.; Nakamura, Y.; Hong, Y.; Mori, S.; Miki, K.; Ohe, K.; Notsuka, Y.; Yamaoka, Y.; Ishida, M.; Kim, D.; Furuta, H. *J. Am. Chem. Soc.* **2020**, *142*, 4429−4437.

(8) (a) Loudet, A.; Burgess, K. *Chem. Rev.* **2007**, *107*, 4891−4932. (b) Ulrich, G.; Ziessel, R.; Harriman, A. *Angew. Chem., Int. Ed.* **2008**, *47*, 1184−1201. (c) Zhao, J.; Xu, K.; Yang, W.; Wang, Z.; Zhong, F. *Chem. Soc. Rev.* **2015**, *44*, 8904−8939. (d) Boens, N.; Verbelen, B.; Ortiz, M. J.; Jiao, L.; Dehaen, W. *Coord. Chem. Rev.* **2019**, *399*, 213024. (e) Qin, W.; Baruah, M.; Van der Auweraer, M.; De Schryver, F. C.; Boens, N. *J. Phys. Chem. A* **2005**, *109*, 7371−7384.

(9) (a) Lu, H.; Mack, J.; Yang, Y.; Shen, Z. *Chem. Soc. Rev.* **2014**, *43*, 4778−4823. (b) Ni, Y.; Wu, J. *Org. Biomol. Chem.* **2014**, *12*, 3774−3791. (c) Wang, J.; Boens, N.; Jiao, L.; Hao, E. *Org. Biomol. Chem.* **2020**, *18*, 4135−4156. (d) Sheng, W.; Lv, F.; Tang, B.; Hao, E.; Jiao, L. *Chin. Chem. Lett.* **2019**, *30*, 1825−1833. (e) Xi, D.; Xiao, M.; Cao, J.; Zhao, L.; Xu, N.; Long, S.; Fan, J.; Shao, K.; Sun, W.; Yan, X.; Peng, X. *Adv. Mater.* **2020**, *32*, 1907855.

(10) (a) Wakamiya, A.; Murakami, T.; Yamaguchi, S. *Chem. Sci.* **2013**, *4*, 1002−1007. (b) Nakamura, M.; Kitatsuka, M.; Takahashi, K.; Nagata, T.; Mori, S.; Kuzuhara, D.; Okujima, T.; Yamada, H.; Nakae, T.; Uno, H. *Org. Biomol. Chem.* **2014**, *12*, 1309−1312. (c) Yu, C.; Jiao, L.; Li, T.; Wu, Q.; Miao, W.; Wang, J.; Wei, Y.; Mu, X.; Hao, E. *Chem. Commun.* **2015**, *51*, 16852−16855. (d) Wang, J.; Wu, Q.; Wang, S.; Yu, C.; Li, J.; Hao, E.; Wei, Y.; Mu, X.; Jiao, L. *Org. Lett.* **2015**, *17*, 5360−5363. (e) Yokoi, H.; Wachi, N.; Hiroto, S.; Shinokubo, H. *Chem. Commun.* **2014**, *50*, 2715−2717. (f) Patalag, L.; Jones, P.; Werz, D. *Angew. Chem., Int. Ed.* **2016**, *55*, 13340−13344. (g) Ke, X.; Kim, T.; Lynch, V.; Kim, D.; Sessler, J. *J. Am. Chem. Soc.* **2017**, *139*, 13950−13956. (h) Kim, T.; Duan, Z.; Talukdar, S.; Lei, C.; Kim, D.; Sessler, J.; Sarma, T. *Angew. Chem., Int. Ed.* **2020**, *59*, 13063−13070. (i) Ni, Y.; Lee, S.; Son, M.; Aratani, N.; Ishida, M.; Samanta, A.; Yamada, H.; Chang, Y.; Furuta, H.; Kim, D.; Wu, J. *Angew. Chem., Int. Ed.* **2016**, *55*, 2815−2819. (j) Shimogawa, H.; Murata, Y.; Wakamiya, A. *Org. Lett.* **2018**, *20*, 5135−5138.

(11) (a) Hayashi, S.; Yamaguchi, W.; Cha, D.; Kim, H.; Shinokubo, H. Shinokubo. *Org. Lett.* **2011**, *13*, 2992−2995. (b) Bruhn, T.; Pescitelli, G.; Jurinovich, S.; Schaumlöffel, A.; Witterauf, F.; Ahrens, J.; Bröring, M.; Bringmann, G. *Angew. Chem., Int. Ed.* **2014**, *53*, 14592−14595.

(12) (a) Ahrens, J.; Haberlag, B.; Scheja, A.; Tamm, M.; Bröring, M. *Chem. - Eur. J.* **2014**, *20*, 2901−2912. (b) Yokoi, Y.; Hiroto, S.; Shinokubo, H. *Org. Lett.* **2014**, *16*, 3004−3007. (c) Xu, L.; Wen, B.; Kim, G.; Kim, T.; Cheng, F.; Zhou, M.; Xu, L.; Tanaka, T.; Yin, B.; Osuka, A.; Kim, D.; Song, J. *Angew. Chem., Int. Ed.* **2017**, *56*, 12322−12326. (d) Ye, S.; Rao, J.; Qiu, S.; Zhao, J.; He, H.; Yan, Z.; Yang, T.; Deng, Y.; Ke, H.; Yang, H.; Zhao, Y.; Guo, Z.; Chen, H. *Adv. Mater.* **2018**, *30*, 1801216. (e) Patalag, L.; Ho, L.; Jones, P.; Werz, D. *J. Am. Chem. Soc.* **2017**, *139*, 15104−15113. (f) Taguchi, D.; Nakamura, T.; Horiuchi, H.; Saikawa, M.; Nabeshima, T. *J. Org. Chem.* **2018**, *83*, 5331−5337. (g) Cakmak, Y.; Akkaya, E. U. *Org. Lett.* **2009**, *11*, 85−88. (h) Zhang, W.; Sheng, W.; Yu, C.; Wei, Y.; Wang, H.; Hao, E.; Jiao, L. *Chem. Commun.* **2017**, *53*, 5318. (i) Saino, S.; Saikawa, M.; Nakamura, T.; Yamamura, M.; Nabeshima, T. *Tetrahedron Lett.* **2016**, *57*, 1629−1634. (j) Sakamoto, N.; Ikeda, C.; Yamamura, M.; Nabeshima, T. *Chem. Commun.* **2012**, *48*, 4818−4820. (k) Tsuchiya, M.; Sakamoto, R.; Shimada, M.; Yamanoi, Y.; Hattori, Y.; Sugimoto, K.; Nishibori, E.; Nishihara, H. *Chem. Commun.* **2017**, *53*, 7509.

(13) (a) Pang, W.; Zhang, X.; Zhou, J.; Yu, C.; Hao, E.; Jiao, L. *Chem. Commun.* **2012**, *48*, 5437−5439. (b) Nepomnyashchii, A.; Bröring, M.; Ahrens, J.; Bard, A. *J. Am. Chem. Soc.* **2011**, *133*, 8633−8645. (c) Cakmak, Y.; Kolemen, S.; Duman, S.; Dede, Y.; Dolen, Y.; Kilic, B.; Kostereli, Z.; Yildirim, L.; Dogan, A.; Guc, D.; Akkaya, E. *Angew. Chem., Int. Ed.* **2011**, *50*, 11937−11941. (d) Kandrashkin, Y.; Wang, Z.; Sukhanov, A.; Hou, Y.; Zhang, X.; Liu, Y.; Voronkova, V.; Zhao, J. *J. Phys. Chem. Lett.* **2019**, *10*, 4157−4163.

(14) Zhou, X.; Yu, C.; Feng, Z.; Yu, Y.; Wang, J.; Hao, E.; Wei, Y.; Mu, X.; Jiao, L. *Org. Lett.* **2015**, *17*, 4632−4635.

(15) Guo, Y.; Li, Y.; Awartani, O.; Han, H.; Zhao, J.; Ade, H.; Yan, H.; Zhao, D. *Adv. Mater.* **2017**, *29*, 1700309.

(16) (a) Roper, D.; Ahn, W.; Hoepfner, M. *J. Phys. Chem. C* **2007**, *111*, 3636. (b) Zou, Q.; Abbas, M.; Zhao, L.; Li, S.; Shen, G.; Yan, X. *J. Am. Chem. Soc.* **2017**, *139*, 1921−1927.

(17) Zhang, Y.; Feng, L.; Wang, J.; Tao, D.; Liang, C.; Cheng, L.; Hao, E.; Liu, Z. *Small* **2018**, *14*, 1802991.

https://dx.doi.org/10.1021/acs.orglett.0c02704
Org. Lett. XXXX, XXX, XXX−XXX